JOURNAL OF GUIDANCE, CONTROL, AND DYNAMICS
Vol. 19, No. 2, March–April 1996

Approximate Initial Lagrange Costates for Continuous-Thrust Spacecraft

James D. Thorne* and Christopher D. Hall†
U.S. Air Force Institute of Technology, Wright–Patterson Air Force Base, Ohio 45433-6583

A method is presented to obtain approximate initial costate values and flight time for the optimal control of a continuous-thrust spacecraft on a coplanar, circle-to-circle transfer. The approximate initial costates are then used as starting values for the associated boundary-value problem to match the desired final states. The exact, nonlinear differential equations are integrated to solve the boundary-value problem with a shooting method. The approximate expressions for the initial costates and flight time are useful when the thrust acceleration is greater than or equal to the change in orbital radius, in canonical units. Numerical examples are provided for a geocentric and an Earth–Mars orbital transfer.

Introduction

NEW propulsion technologies have raised interest in the space community for continuous-thrust orbital missions. In military applications, this could mean more responsive deployment of space assets and longer on-orbit lifetimes. Tactical repositioning of a satellite using chemical propulsion can consume large amounts of the available fuel mass per maneuver. This is certainly unacceptable for many reasons including lifetime, reliability, and cost. A spacecraft propelled by high-efficiency thrusters could accomplish many more maneuvers for the same amount of fuel mass as a chemical propulsion system.

Another interesting application of continuous-thrust propulsion is interplanetary space travel. A permanently orbiting space station could serve as a launch point for solar system exploration. Maintaining cryogenic fuels for this purpose, however, would be technically difficult and extremely costly. These problems would be less significant if the orbiting space station were used as an assembly point for an exploration vehicle propelled by high-efficiency continuous thrusters. Such a vehicle could be made reusable much more easily in terms of reliability and cost than a chemically propelled spacecraft. Also, a vehicle using continuous thrust with existing technology could shorten travel times compared to fuel-optimal impulsive maneuvers, then could return to Earth orbit for reconditioning.

Although the optimization of impulsive transfers has a direct solution,[1] none has been found for the continuous-thrust case. This problem may be solved numerically, and many examples of this are to be found in the literature.[2] Optimization of a continuous-thrust trajectory involves the simultaneous solution of an optimal control problem and a boundary-value problem. The initial and final states are normally known, but there is usually no information available for the initial values of the Lagrange costates. This presents quite a problem, since the optimal control law is often a function of the Lagrange costates that must be initialized for numerical integration. The usual approach is to make an educated guess for the initial values, then update them by solving the boundary-value problem. Prussing,[3] Broucke,[4] and others[2] have recast the boundary-value problem in terms of other variables, but the initial values of these must be guessed and refined as well. Prussing[3] incorporated the second derivative of the primer vector into a fourth-order dynamics equation, thus eliminating the control variables. Once this is accomplished, four constants of integration must be iterated to find the correct optimal trajectory. Broucke[4] expressed the Lagrange multipliers as functions of new auxiliary variables and graphically examined the behavior of the new variables.

Pines[5] suggested using the results of optimal impulsive maneuvers to serve as an initial guess for the continuous-thrust case. However, this method produces poor results for small values of continuous thrust, particularly if there are no coasting arcs used. Coasting arcs appear in the optimal fuel solution for continuous-thrust vehicles when the switching function changes sign.[6]

Closed-form nonoptimal solutions have been found for spacecraft trajectories where special assumptions are made about the control law. If the thrust vector is directed either radially away from the attracting center or tangentially to the orbital path, it is possible to integrate the equations of motion analytically. Battin[7] presents results for the time to reach escape velocity and the number of revolutions for both thrust assumptions.

Assumptions about the thrust magnitude will also allow closed-form nonoptimal solutions through the method of averaging. If the thrust level is small enough, there is only a small change in semimajor axis or eccentricity for a single orbital revolution. Then, a correction is made to the semimajor axis at the completion of each revolution. These approximations are reasonable for orbital transfers that require roughly 10 or more revolutions to complete.[8,9] Using these assumptions, it is possible to solve analytically for the approximate trajectory. The thrust is directed tangentially; this is also perpendicular to the orbit radius because the eccentricity is assumed to be zero for individual revolutions.

For circle-to-circle coplanar orbital transfers, the minimum time of flight may be derived from the accumulated velocity change (integrated ΔV) on the trajectory. It is possible to display the optimal accumulated velocity change in graphical form for a large range of constant thrust levels, ratio of final to initial orbit radius, and mass propellant fraction.[10] In this way, a wide range of possible cases may be represented through the use of canonical variables. To produce the graphical results, many different cases must be solved numerically to allow for interpolation. Although linear interpolation from a graph will not provide great precision, it does show general trends for mission design. In particular, a graph of the number of revolutions for the optimal path vs the logarithm of thrust magnitude shows a distinct change in trajectory characteristics at integer values of revolutions.[10]

Our goal is to develop analytical expressions for the approximate values of the optimal initial costates and time of flight for the minimum time, circle-to-circle orbital transfer. These values are then to be used as initial guesses for the associated boundary-value problem with no approximations. This way, the final result is a converged boundary-value problem that produces the truly optimal control law, instead of an exact solution to some suboptimal approach with an assumed control history.

Presented as AAS Paper 95-119 at the AAS/AIAA Space Flight Mechanics Meeting, Albuquerque, NM, Feb. 13–16, 1995; received March 24, 1995; revision received Oct. 3, 1995; accepted for publication Oct. 30, 1995.

*Doctoral Candidate, Department of Aeronautics and Astronautics.
†Assistant Professor of Aerospace and Systems Engineering, Department of Aeronautics and Astronautics. Senior Member AIAA.

To find the analytical expressions, the equations of motion are modified by neglecting the gravitational term. The resulting differential equations for the states and costates are integrated analytically to produce algebraic equations of motion. Two of the constants of integration are the desired initial costate values. When boundary conditions are introduced, the initial costates are then expressed as functions of canonical parameters. The useful range of the approximate expressions is discussed, and numerical examples are given.

Equations of Motion

The optimal control law for a continuously thrusting spacecraft may be found using variational calculus techniques.[11] Figure 1 shows the Cartesian coordinates x_1 and x_2 and the problem geometry. The acceleration resulting from thrust is A, the gravitational parameter is μ, and the velocities in the x_1 and x_2 directions are v_1 and v_2, respectively. The length of the position vector is r, and the final desired value of r will be given by R.

The minimum time to R is found by repeatedly maximizing the final radius for different flight times, then choosing the time such that the final radius is R. Since time is the independent variable, a final value of the time makes a reliable stopping condition for integrating the equations of motion. However, the stopping condition $r = R$ is not reliable, since r may decrease for some initial conditions of the costates. Therefore, maximizing R for a given flight time is the most practical approach to the problem.

This approach leads to the following variational Hamiltonian[6]:

$$\mathcal{H}_c = \lambda_{x_1} v_1 + \lambda_{x_2} v_2 + \lambda_{v_1}\left[-(\mu/r^3)x_1 + A\cos\phi\right] + \lambda_{v_2}\left[-(\mu/r^3)x_2 + A\sin\phi\right] \tag{1}$$

The associated costates are represented by λ and are also known as Lagrange multipliers. From the Hamiltonian, one may obtain[6] a set of first-order differential equations for each of the states and costates, as well as the optimal control law. The control law that maximizes the radius for a given flight time is found by setting $\partial\mathcal{H}_c/\partial\phi = 0$ and leads to

$$\phi = \tan^{-1}\left(\lambda_{v_2}/\lambda_{v_1}\right) \tag{2}$$

One may choose various values of flight time to match the desired final radius through a shooting method. Once the end conditions have been met, the resulting time of flight will be the minimum necessary to reach the desired radius.[6] In this case, the second derivative of the Hamiltonian with respect to the thrust angle ϕ will be negative, which meets the Legendre–Clebsch condition for a maximum.

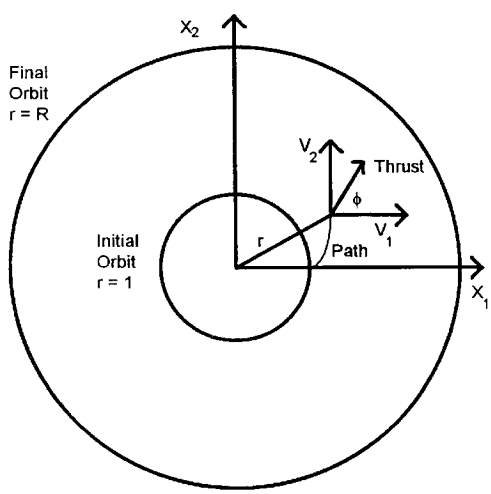

Fig. 1 Problem geometry with flight path.

Using the control law, the equations of motion in Cartesian coordinates are as follows:

$$\dot{x}_1 = v_1 \tag{3}$$

$$\dot{x}_2 = v_2 \tag{4}$$

$$\dot{v}_1 = -\frac{\mu}{r^3}x_1 + A\left(\frac{\lambda_{v_1}}{\sqrt{\lambda_{v_1}^2 + \lambda_{v_2}^2}}\right) \tag{5}$$

$$\dot{v}_2 = -\frac{\mu}{r^3}x_2 + A\left(\frac{\lambda_{v_2}}{\sqrt{\lambda_{v_1}^2 + \lambda_{v_2}^2}}\right) \tag{6}$$

$$\dot{\lambda}_{x_1} = -\frac{\mu}{r^3}\left[\left(\frac{3x_1^2}{r^2} - 1\right)\lambda_{v_1} + \frac{3x_1x_2}{r^2}\lambda_{v_2}\right] \tag{7}$$

$$\dot{\lambda}_{x_2} = -\frac{\mu}{r^3}\left[\left(\frac{3x_2^2}{r^2} - 1\right)\lambda_{v_2} + \frac{3x_1x_2}{r^2}\lambda_{v_1}\right] \tag{8}$$

$$\dot{\lambda}_{v_1} = -\lambda_{x_1} \tag{9}$$

$$\dot{\lambda}_{v_2} = -\lambda_{x_2} \tag{10}$$

$$A = \frac{T}{m_0 + \dot{m}t} \tag{11}$$

Once the control law has been determined as a function of Lagrange multipliers, a boundary-value problem must be solved to meet the desired end conditions. This technique requires initial values for each of the states and costates. However, the initial values of the costates are generally unknown. Thus, they must be guessed and refined to solve the problem using some numerical technique such as the shooting method.[12] We will present an approximate closed-form solution for the initial costate values as a function of spacecraft thrust acceleration A and the final circular orbit radius R. The problem we will consider is optimal planar transfer from one circular orbit defined with radius = 1 to a larger circular orbit of radius = R under continuous thrust. The problem of transferring to a lower orbit may be recast as an equivalent orbit-raising problem by defining the canonical distance unit with the final orbit radius that would be smaller in that case and using a negative time step.

Zero-Gravity Approximation

In canonical units,[13] the gravitational constant μ is unity regardless of the system under consideration as long as the initial circular radius is defined to be one distance unit (DU) and the initial circular velocity is one distance unit per time unit (DU/TU). If the equations of motion are approximated by setting $\mu = 0$ and $\dot{m} = 0$, the differential equations for the states and costates may be integrated in closed form. Although ignoring the gravity may not seem to be the most obvious choice for approximation, it does reduce the problem to a system of algebraic equations. Further, the boundary conditions are still chosen to be circular orbits. Thus, gravity still has an influence on the solution since the boundary conditions are a function of the nominal gravitational constant value, $\mu = 1$. A mass flow rate of zero is not realistic for any real propulsion system, but it can have a surprisingly small effect on the optimal initial costate values as will be shown by example.

Once these two approximations ($\mu = 0$, $\dot{m} = 0$) have been made, the equations of motion in Cartesian coordinates simplify enough to allow analytical integration. The result is a system of eight algebraic equations for the position and velocity components and their associated costates. These solutions are functions of the constant-thrust acceleration A, final orbit radius R, time, and various constants of integration.

Setting the gravitational constant to zero, the differential equations of motion simplify to

$$\dot{x}_1 = v_1 \tag{12}$$

$$\dot{x}_2 = v_2 \tag{13}$$

$$\dot{v}_1 = A\left(\frac{\lambda_{v_1}}{\sqrt{\lambda_{v_1}^2 + \lambda_{v_2}^2}}\right) \tag{14}$$

$$\dot{v}_2 = A\left(\frac{\lambda_{v_2}}{\sqrt{\lambda_{v_1}^2 + \lambda_{v_2}^2}}\right) \tag{15}$$

$$\dot{\lambda}_{x_1} = 0 \tag{16}$$

$$\dot{\lambda}_{x_2} = 0 \tag{17}$$

$$\dot{\lambda}_{v_1} = -\lambda_{x_1} \tag{18}$$

$$\dot{\lambda}_{v_2} = -\lambda_{x_2} \tag{19}$$

The last four equations may be integrated immediately and substituted into the first four equations. Defining $\lambda_x = \sqrt{(\lambda_{x_1}^2 + \lambda_{x_2}^2)}$, and $\lambda_v = \sqrt{(\lambda_{v_1}^2 + \lambda_{v_2}^2)}$, the $\mu = 0$ solutions are

$$\lambda_{x_1} = a \tag{20}$$

$$\lambda_{x_2} = b \tag{21}$$

$$\lambda_{v_1} = -at + c \tag{22}$$

$$\lambda_{v_2} = -bt + d \tag{23}$$

$$\begin{aligned} x_1 = {} & A\left[\left(\lambda_v/2\lambda_x^4\right)\left(a^2c - 2b^2c + 3abd - a\lambda_x^2 t\right)\right. \\ & + \left(1/2\lambda_x^5\right)\left(-3ab^2c^2 + 4a^2bcd - 2b^3cd\right. \\ & - a^3d^2 + 2ab^2d^2 + 2\lambda_x^2 b(bc - ad)t\Big) \\ & \left.\times \ell_n\left(-ac - bd + \lambda_x^2 t + \lambda_x\lambda_v\right)\right] + k_1 t + k_3 \end{aligned} \tag{24}$$

$$\begin{aligned} x_2 = {} & A\left[\left(\lambda_v/2\lambda_x^4\right)\left(b^2d - 2a^2d + 3abc - b\lambda_x^2 t\right)\right. \\ & + \left(1/2\lambda_x^5\right)\left(-3a^2bd^2 + 4ab^2cd - 2a^3cd\right. \\ & - b^3c^2 + 2a^2bc^2 + 2\lambda_x^2 a(ad - bc)t\Big) \\ & \left.\times \ell_n\left(-ac - bd + \lambda_x^2 t + \lambda_x\lambda_v\right)\right] + k_2 t + k_4 \end{aligned} \tag{25}$$

$$\begin{aligned} v_1 = {} & \left(A/\lambda_x^3\right)\left[-a\lambda_x\lambda_v + b(bc - ad)\right. \\ & \left.\times \ell_n\left(-ac - bd + \lambda_x^2 t + \lambda_x\lambda_v\right)\right] + k_1 \end{aligned} \tag{26}$$

$$\begin{aligned} v_2 = {} & \left(A/\lambda_x^3\right)\left[-b\lambda_x\lambda_v + a(ad - bc)\right. \\ & \left.\times \ell_n\left(-ac - bd + \lambda_x^2 t + \lambda_x\lambda_v\right)\right] + k_2 \end{aligned} \tag{27}$$

The terms a, b, c, d, k_1, k_2, k_3, and k_4 are constants of integration. Because the Lagrange multipliers appear in the Hamiltonian as linear terms, the initial value of one of them may be scaled to unity. For this system, we choose $\lambda_{x_1}(0) = 1$; thus, $a = 1$. Also, if the initial state is on a circular orbit, we have $b = c$. This may be seen by equating the system Hamiltonian expressed in polar and Cartesian coordinates. The polar coordinates include r as the scalar distance from the attracting center, u as the time rate of change of r, and w as the velocity component perpendicular to u, directed along the spacecraft horizon. Here, the Hamiltonian is expressed in both sets of coordinates

$$\begin{aligned} \mathcal{H}_p = {} & \lambda_r u + \lambda_u[(w^2/r) - (\mu/r^2) + A\cos\phi] \\ & + \lambda_w[-(uw/r) + A\sin\phi] \end{aligned} \tag{28}$$

$$\begin{aligned} \mathcal{H}_c = {} & \lambda_{x_1} v_1 + \lambda_{x_2} v_2 + \lambda_{v_1}[-(\mu/r^3)x_1 + A\cos\phi] \\ & + \lambda_{v_2}[-(\mu/r^3)x_2 + A\sin\phi] \end{aligned} \tag{29}$$

The initial conditions for the polar and Cartesian cases are

$$r(0) = 1 \qquad u(0) = 0 \qquad w(0) = 1$$

$$x_1(0) = 1 \qquad x_2(0) = 0 \qquad v_1(0) = 0 \qquad v_2(0) = 1$$

Using these initial conditions and equating the resulting Hamiltonians yields

$$\lambda_u A\cos\phi + \lambda_w A\sin\phi = \lambda_{x_2} + \lambda_{v_1}(-1 + A\cos\phi) + \lambda_{v_2} A\sin\phi \tag{30}$$

By equating coefficients of $\sin\phi$ and $\cos\phi$, the following three relationships are obtained:

$$\lambda_{x_2}(0) = \lambda_{v_1}(0)\ (= b = c) \tag{31}$$

$$\lambda_{v_1}(0) = \lambda_u(0)\ (= b) \tag{32}$$

$$\lambda_{v_2}(0) = \lambda_w(0)\ (= d) \tag{33}$$

The constants k_1 and k_2 may be eliminated from Eqs. (24–27) by using the velocity component end conditions v_{10}, v_{1f}, v_{20}, and v_{2f} and the final time t_f. This yields

$$\frac{(v_{1f} - v_{10})\lambda_x^3}{A} = \lambda_x(\lambda_{v0} - \lambda_{vf}) + b(d - b^2)L \tag{34}$$

$$\frac{(v_{2f} - v_{20})\lambda_x^3}{Ab} = \lambda_x(\lambda_{v0} - \lambda_{vf}) + \left(\frac{b^2 - d}{b}\right)L \tag{35}$$

$$L = \ell_n\left(\frac{-b - bd + \lambda_x\lambda_{v0}}{-b - bd + \lambda_x\lambda_{v0} + \lambda_x^2 t_f}\right) \tag{36}$$

In the special case where the initial and final velocity components are all equal to zero, the optimal trajectory is a straight line. If $\dot{m} = 0$, the thrust will switch directions midway through the trajectory to decelerate to a stop, and the time of flight is $t_f = 2\sqrt{[(R-1)/A]}$. This straight-line case allows for a simplification of the preceding equations. They take the form

$$\lambda_x(\lambda_{v0} - \lambda_{vf}) + b(d - b^2)L = 0 \tag{37}$$

$$\lambda_x(\lambda_{v0} - \lambda_{vf}) + [(b^2 - d)/b]L = 0 \tag{38}$$

The only difference in the two preceding equations is the coefficient of the logarithmic term, and so these coefficients must be equal. This leads to the following relationship:

$$(b^2 + 1)(d - b^2) = 0 \tag{39}$$

Clearly, the real solution is $d = b^2$. If this result is substituted back into Eq. (37), the logarithmic term vanishes. Since $\lambda_x \geq 1$ by definition, we have

$$\lambda_{v0} = \lambda_{vf} \tag{40}$$

Using the definition $\lambda_v = \sqrt{(\lambda_{v_i}^2 + \lambda_{v_2}^2)}$ and the solutions for λ_{v_1} and λ_{v_2} given in Eqs. (22) and (23), this becomes

$$\sqrt{b^2 + d^2} = \sqrt{(b - t_f)^2 + (d - bt_f)^2} \tag{41}$$

Squaring both sides, expanding, and collecting terms leads to

$$-2b^3 + t_f b^2 - 2b + t_f = 0 \tag{42}$$

$$(b^2 + 1)(b - t_f/2) = 0 \tag{43}$$

Again taking the real solution, the result is $b = t_f/2$. Using this and the results for b and d, we have the complete solution to the straight-line case

$$b_0 = \sqrt{(R-1)/A} \tag{44}$$

$$d_0 = (R-1)/A \tag{45}$$

$$t_{f0} = 2\sqrt{(R-1)/A} \tag{46}$$

where the zero subscript indicates that these solutions are for the simplest case of no gravity, no mass flow rate, and zero velocity end conditions. Note that $\lambda_{v_1} = b_0$ and $\lambda_{v_2} = d_0$ define a parabola in the $\lambda_{v_2}, \lambda_{v_1}$ plane.

Equations (44–46) along with $b = c$ and $a = 1$ provide an approximate analytical solution for the initial values of the Lagrange costates and the final time. These approximations can be used to start suboptimal transfers, or as starting points for solving the two-point boundary-value problem. Further refinement is possible by scaling these results, as will be shown next.

In Fig. 2, the exact initial costates for the zero-gravity case are shown on the solid line. These are obtained by numerically solving the $\mu = 0 = \dot{m}$ two-point boundary-value problem with circular end conditions corresponding to an Earth–Mars transfer ($R = 1.525$). The ○ symbols correspond to A values of 1000, 100, 10, and 1.6, with the largest values near the origin. Initial costate values for $A < 1.6$ do not lie near a parabolic arc for $R = 1.525$. The dashed line is a parabola defined by Eqs. (44) and (45) for $b_0 = \lambda_{v_1}(0)$ and $d_0 = \lambda_{v_2}(0)$. The × symbols correspond to the same values of A as the ○ symbols. Note the excellent agreement for large A as expected. A simple scaling approach leads to improved agreement for the lower values of A. The scaled points are shown with the + symbols, and the scaling factor q is defined as follows:

$$b \approx q\sqrt{(R-1)/A} \tag{47}$$

$$d \approx q^2[(R-1)/A] \tag{48}$$

The time of flight t_f is not as sensitive to the presence of the gravity term, and so the formula for t_f does not require additional scaling.

If the two velocity components, Eqs. (26) and (27), are used to eliminate their common logarithmic term, the following relationship is obtained:

$$\left(\frac{v_{1f} - v_{10}}{A}\right) + b\left(\frac{v_{2f} - v_{20}}{A}\right) + \sqrt{(b - t_f)^2 + (d - bt_f)^2} - \sqrt{b^2 + d^2} = 0 \tag{49}$$

The initial velocity components are $v_{10} = 0$ and $v_{20} = 1$ on the starting circular orbit. The final Cartesian velocity components are not known individually at t_f, and they may be set equal to zero as an approximation. In this way, the scaling factor may be introduced

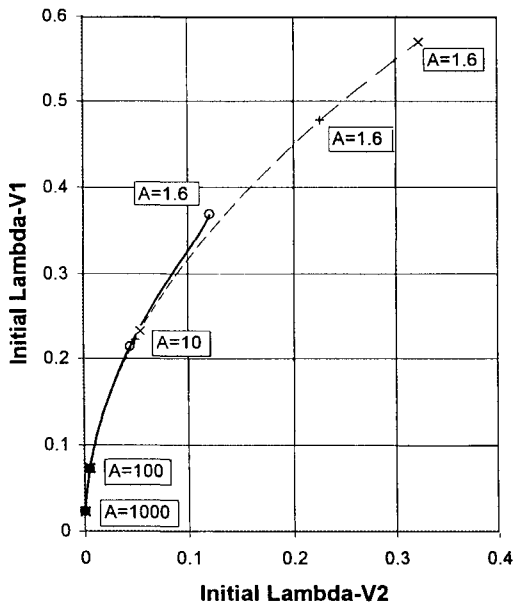

Fig. 2 Comparison of various costate solutions. $R = 1.525$, $\mu = 0$, $\dot{m} = 0$: ——, exact values, circular B.C.s; – – –, parabolic arc; ×, unscaled approximations; +, scaled approximations; and ○, exact values, circular B.C.s.

to produce an equation in a single variable with two parameters, R and A. Let $s = \sqrt{[(R-1)/A]}$. Then, Eq. (49) becomes

$$-(qs/A) + \sqrt{(q-2)^2 s^2 + (q^2 s^2 - 2qs^2)^2} - \sqrt{q^2 s^2 + q^4 s^4} = 0 \tag{50}$$

The scaling factor q may be expressed as an infinite series in the quantity $(1/A)$. After solving for the coefficients, the first three terms in this series solution are

$$q \approx 1 - (1/2A) + (R/4A^2) \tag{51}$$

Using this result, the initial costates are given by

$$b \approx \left(1 - \frac{1}{2A} + \frac{R}{4A^2}\right)\sqrt{\frac{R-1}{A}} \qquad [= \lambda_{v_1}(0)] \tag{52}$$

$$d \approx \left(1 - \frac{1}{2A} + \frac{R}{4A^2}\right)^2\left(\frac{R-1}{A}\right) \qquad [= \lambda_{v_2}(0)] \tag{53}$$

Since the expansion for q involves the quantity $(1/A)$, it should not be used if $A < 1$. If $A < 1$, the approximate initial costates may be obtained from Eqs. (44) and (45), which do not include the scaling factor q.

To summarize, Eqs. (44) and (45) give the approximate initial costate values, and Eq. (46) is the approximate time of flight. If $A > 1$, the scaled Eqs. (52) and (53) should be used to improve the approximate initial costate values. These relationships were derived using the assumptions of zero gravity, zero mass flow rate, and zero final velocity components. Even using these assumptions, the results lead to a good initial guess for the associated boundary-value problem over a large range of problem parameters.

It has been found from numerical studies that the ratio of the radius change to the thrust acceleration, $(R-1)/A$, must be equal to one or less in canonical units for the approximate initial costates to provide a reasonable first guess.

Numerical Examples

Two numerical examples will be given to illustrate geocentric and heliocentric missions. The trajectories were propagated with an integration tolerance of 10^{-8} and an error tolerance in the final state values of 10^{-7} in canonical units.

Example 1 involves a spacecraft design that has been investigated by past researchers.[14] A 2400-kg spacecraft is at geosynchronous altitude with a thrust of 1.3 N and a mass flow rate of −0.000069 kg/s. In canonical units, the problem parameters are $A = 0.002425$ and $\dot{m} = -0.000395$. Suppose that it is desired to make a small increase in altitude in minimum time to avoid a ballistic antisatellite weapon. If $R = 1.000336$, the new orbit radius will increase by roughly 15 km. Using the given problem parameters, the results in canonical units are given in Table 1.

The first line in Table 1 is the set of converged values for example 1 that includes the effects of gravity and mass flow rate. The second line shows the values obtained by using the approximate solutions from Eqs. (44–46), where $\lambda_{v_1}(0) = b$ and $\lambda_{v_2}(0) = d$. The zeros listed for μ and $\dot{m}$ are a reminder that the approximate solutions were derived with these assumptions. The scaling factor q was not used in this example since $A < 1$. The total thrusting time is roughly 2.8 h.

Figure 3 shows the iterative search history for the flight time and initial costates in example 1 from the initial guess to the converged values. In this case, the initial estimates were very close to the final values, so that convergence was achieved in four iterations of the shooting method. Figure 4 compares the exact control angle history from the converged case with the approximate history generated

Table 1 Results from example 1

μ	$\dot{m}$	t_f	$\lambda_{v_1}(0)$	$\lambda_{v_2}(0)$
1	−0.000395	0.7366198	0.3395791	0.1201369
0	0	0.7441893	0.3720947	0.1384544

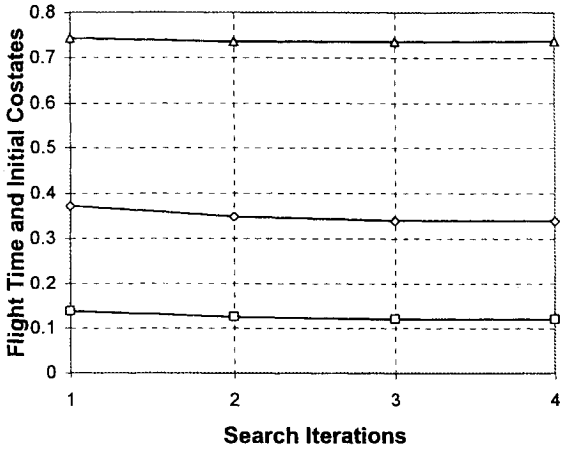

Fig. 3 Iterative search history for example 1. R = 1.000336, A = 0.002425: —△—, time of flight; —◇—, $\lambda_{v_1}(0)$; and —□—, $\lambda_{v_2}(0)$.

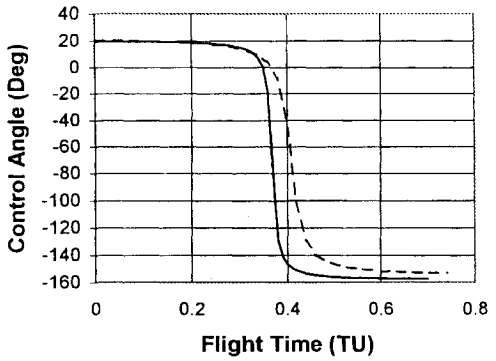

Fig. 4 Control angle history for example 1. R = 1.000336, A = 0.002425: ——, exact values and – – –, approximate values.

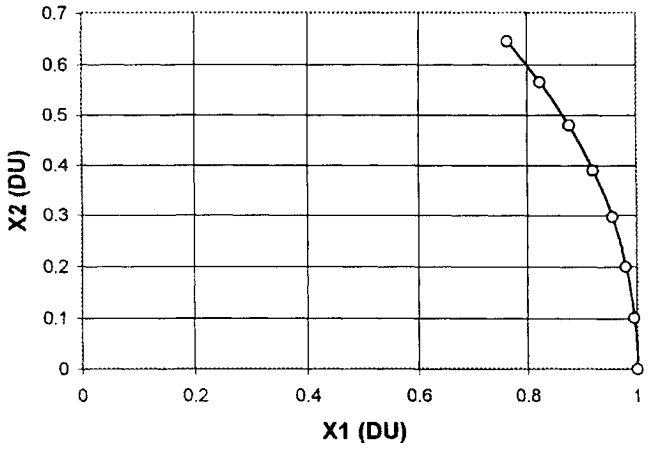

Fig. 5 Trajectories using exact and approximate λ_0 for example 1. R = 1.000336, A = 0.002425: ——, exact path and o, approximate path.

by the initial estimates. Both curves pass through the zero angle, showing the switch in thrust direction. The differences between the initial estimates and the converged values are most evident here, since the costate histories are very sensitive to the initial conditions.

Figure 5 shows a comparison of flight-path trajectories using the control law from the initial estimates and the converged values. In this case, the paths are almost identical in spite of the differences in the control-angle histories.

The second example is an Earth–Mars transfer, with $A = 1$ and $\dot{m} = -0.5$. These parameters are each roughly seven times greater than those given in the well-known example from Bryson and Ho.[6] A high-performance spacecraft with these parameters might have an array of thrusters with a common fuel source, as well as reasonable improvements in the power generation system. There is, however,

Table 2 Results from example 2

μ	$\dot{m}$	t_f	$\lambda_{v_1}(0)$	$\lambda_{v_2}(0)$
1	−0.5	1.1699013	0.5312363	0.3737511
0	0	1.4491376	0.6385263	0.4077158

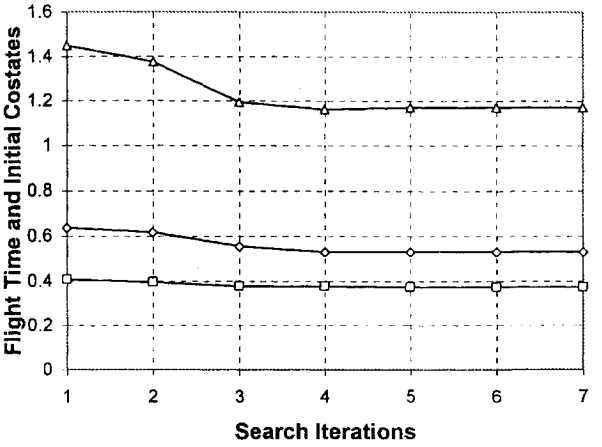

Fig. 6 Search history for example 2. R = 1.525, A = 1, $\dot{m}$ = −0.5: —△—, time of flight; —◇—, $\lambda_{v_1}(0)$; and —□—, $\lambda_{v_2}(0)$.

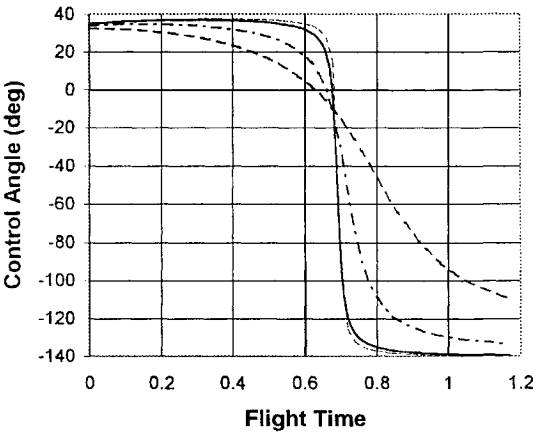

Fig. 7 Control-angle history for example 2. R = 1.525, A = 1, $\dot{m}$ = −0.5: ——, exact values; – – –, first approximation; – – –, second approximation; and - - - -, third approximation.

no assumed improvement in the specific impulse compared to the classic example. Using the given problem parameters, the results in canonical units are given in Table 2.

The first line in Table 2 is the set of converged values for example 2 that includes the effects of gravity and mass flow rate. The second line shows the values obtained by using the approximate solutions from Eqs. (52) and (53) and Eq. (46), where $\lambda_{v_1}(0) = b$ and $\lambda_{v_2}(0) = d$. The zeros listed for μ and $\dot{m}$ are a reminder that the approximate solutions were derived with these assumptions. The scaling factor $q = 0.88215$ was used in this example, since $A \geq 1$. The total trip time from Earth to Mars is roughly 68 days.

Figure 6 shows the iterative search history for the flight time and initial costates in example 2 from the initial guess to the converged values. In this case, the initial estimates were not as close to the final values as in example 1, and so convergence was achieved in seven iterations of the shooting method.

Figure 7 compares the exact control-angle history from the converged case with the approximate histories generated by the initial estimates of several intermediate values. All curves pass through the zero angle, showing the switch in thrust direction. The initial values were taken from iteration numbers 1, 2, 3, and 7 from the shooting method, to show the refinement process. With each iteration, the approximate control-angle history lies closer to the converged control-angle history.

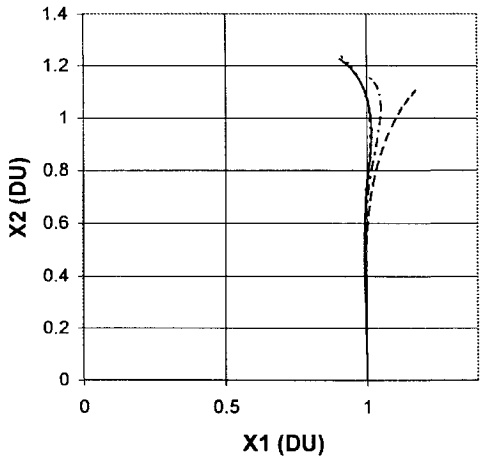

Fig. 8 Trajectories using exact and approximate λ_0 for example 2. $R = 1.525$, $A = 1$, $\dot{m} = -0.5$: ——, exact path; – – –, first approximation; – – – –, second approximation; and - - - -, third approximation.

Figure 8 shows a comparison of flight-path trajectories using the control law from several initial estimates and the converged values. In this case, the flight trajectory from the first estimate is off by roughly 0.3 DU. Again using the intermediate values from iterations 2, 3, and 7, the paths come closer to the converged path with each iteration.

As stated before, it has been found from numerical studies that the ratio of the radius change to the thrust acceleration, $(R-1)/A$, must be equal to one or less in canonical units for the approximate initial costates to provide a reasonable first guess. In example 1, $(R-1)/A = 0.1384544$, and in example 2, $(R-1)/A = 0.4077158$. Since the ratio in example 1 was smaller, the approximate initial values were better. This behavior has been consistent in all cases studied.

The physical implication of the limit $(R-1)/A \leq 1$ is that the orbital transfer will occur in less than one revolution. This is an intuitive result, since the approximation of $\mu = 0$ removes the effect of gravity from the equations of motion. Without gravity, there cannot be periodic, multiple revolution solutions. Therefore, this method works best for transfers of less than one revolution, especially if the path lies in a single quadrant. For problems with more than 10 revolutions, it is well known that the optimal thrust direction is nearly tangential to the path through most of the transfer.[8] For such cases, a good starting guess is $\lambda_{v_1}(0) = 0$ and $\lambda_{v_2}(0) = 1$, although difficulties can always arise because of the sensitive nature of the equations of motion and costates.

Unlike multiple revolution problems, the approximate initial costates for transfers of less than one revolution do not have a well-known limiting case. As shown in the examples, the expressions presented for the approximate initial costates and time of flight will provide a good starting point to solve this type of problem, regardless of the thrust level.

Conclusion

Approximate solutions have been obtained for the initial costate values and flight time for the optimal control of a continuous-thrust spacecraft on a coplanar, circle-to-circle orbital transfer. The method works best for transfers of less than one revolution, particularly if the path lies in a single quadrant. There is no specific limit on thrust level; however, the ratio of the radius change to the thrust acceleration should be less than one in canonical units.

Acknowledgments

The authors would like to acknowledge contributions made by the various reviewers of this work, as well as suggestions made by William E. Wiesel of the U.S. Air Force Institute of Technology.

References

[1]Lawden, D. F., *Optimal Trajectories for Space Navigation*, Butterworths, London, 1963, Chap. 6.

[2]Bell, D. J., "Optimal Space Trajectories—A Review of Published Work," *Aeronautical Journal of the Royal Aeronautical Society*, Vol. 72, No. 686, 1968, pp. 141–146.

[3]Prussing, J. E., "Equation for Optimal Power-Limited Spacecraft Trajectories," *Journal of Guidance, Control, and Dynamics*, Vol. 16, No. 2, 1993, pp. 391–393.

[4]Broucke, R. A., "Low-Thrust Trajectory Optimization in an Inverse Square Force Field," AAS/AIAA Spaceflight Mechanics Meeting, Houston, TX, Feb. 1991, AAS Paper 91-159.

[5]Pines, S., "Constants of the Motion for Optimal Thrust Trajectories in a Central Force Field," *AIAA Journal*, Vol. 2, No. 11, 1964, pp. 2010–2014.

[6]Bryson, A. E., and Ho, Y. C., *Applied Optimal Control*, Hemisphere, Washington, DC, 1975, pp. 66–69.

[7]Battin, R. H., *Astronautical Guidance*, McGraw–Hill, New York, 1964, pp. 70–75.

[8]Alfano, S., "Low Thrust Orbit Transfer," M.S. Thesis, U.S. Air Force Inst. of Technology, AFIT/GA/AA/82D-2, Wright–Patterson AFB, OH, Dec. 1982.

[9]Wiesel, W. E., and Alfano, S., "Optimal Many-Revolution Orbit Transfer," *Journal of Guidance, Control, and Dynamics*, Vol. 8, No. 1, 1985, pp. 155–157.

[10]Alfano, S., and Thorne, J. D., "Constant-Thrust Orbit-Raising," *Journal of the Astronautical Sciences*, Vol. 42, No. 1, 1994, pp. 35–45.

[11]Kirk, D. E., *Optimal Control Theory—An Introduction*, Prentice–Hall, Englewood Cliffs, NJ, 1970, Chap. 5.

[12]Press, W. H., Flannery, B. P., Teukolsky, S. A., and Vettering, W. T., *Numerical Recipes in C—The Art of Scientific Computing*, Cambridge Univ. Press, Cambridge, England, UK, 1988, Chap. 16.

[13]Bate, R., Mueller, D., and White, J., *Fundamentals of Astrodynamics*, Dover, New York, 1971, pp. 40–43.

[14]Eide, S. A., "Optimal Thrust Vector Control of Coplanar Orbital Evasive Maneuvers," M.S. Thesis, U.S. Air Force Inst. of Technology, AFIT/GA/AA/87D-2, Wright–Patterson AFB, OH, Dec. 1987, p. 42.